



RESEARCH LETTER

10.1002/2016GL068950

Key Points:

- A global warming hiatus is extremely unlikely given the current global warming climate
- The likelihood of a hiatus decreases under increasing global warming
- The likelihood of a surge in temperature does not change under increasing global warming

Supporting Information:

- Supporting Information S1

Correspondence to:

F. Sévellec,
florian.sevellec@noc.soton.ac.uk

Citation:

Sévellec, F., B. Sinha, and N. Skliris (2016), The rogue nature of hiatuses in a global warming climate, *Geophys. Res. Lett.*, 43, 8169–8177, doi:10.1002/2016GL068950.

Received 11 JAN 2016

Accepted 15 JUL 2016

Accepted article online 22 JUL 2016

Published online 8 AUG 2016

©2016. The Authors.

This is an open access article under the terms of the Creative Commons Attribution License, which permits use, distribution and reproduction in any medium, provided the original work is properly cited.

The rogue nature of hiatuses in a global warming climate

F. Sévellec¹, B. Sinha², and N. Skliris¹

¹Ocean and Earth Science, University of Southampton, Southampton, UK, ²National Oceanography Centre, Southampton, UK

Abstract The nature of rogue events is their unlikelihood and the recent unpredicted decade-long slowdown in surface warming, the so-called hiatus, may be such an event. However, given decadal variability in climate, global surface temperatures were never expected to increase monotonically with increasing radiative forcing. Here surface air temperature from 20 climate models is analyzed to estimate the historical and future likelihood of hiatuses and “surges” (faster than expected warming), showing that the global hiatus of the early 21st century was extremely unlikely. A novel analysis of future climate scenarios suggests that hiatuses will almost vanish and surges will strongly intensify by 2100 under a “business as usual” scenario. For “CO₂ stabilisation” scenarios, hiatus, and surge characteristics revert to typical 1940s values. These results suggest to study the hiatus of the early 21st century and future reoccurrences as rogue events, at the limit of the variability of current climate modelling capability.

1. Introduction

In the early 21st century, the measured trend in global surface atmospheric temperature (SAT) was significantly reduced compared to previous decades [Trenberth and Fasullo, 2013; IPCC, 2013]. This recent unpredicted hiatus has led to an increasing body of work focused on understanding it [Meehl et al., 2011; Katsman and Oldenborgh, 2011; Watanabe et al., 2013; Meehl et al., 2013; Balmaseda et al., 2013; Maher et al., 2014; Clement and DiNezio, 2014; Drijfhout et al., 2014; England et al., 2014, 2015; Rajaratnam et al., 2015]. Simultaneously, it has raised questions outside the climate research community, to the extent of questioning the very existence of global warming on a part of the public. On the other hand, because of the existence of decadal climate variability, the hiatus was never really a surprise for the more specialized community [Easterling and Wehner, 2009]. Indeed, a cooling trend related to the decadal variability of the climate system can overtake the long-term global warming trend, leading to a hiatus period for a decade or so [Guemas et al., 2013; Trenberth, 2015]. Following the null hypothesis of climate variability (i.e., SAT has a white noise distribution), we can schematically explain the likelihood of a decadal hiatus as the ratio of the intensity of (internally generated) decadal climate variability to the intensity of the (externally forced) global warming trend (Figure 1). Hence, in the context of global warming, the relevant scientific question does not seem to be about the existence of a hiatus but rather seem to be about its likelihood [Maher et al., 2014; Schurer et al., 2015; Roberts et al., 2015; Risbey et al., 2015; Medhaug and Drange, 2015]. This is what we investigate here.

In this study we determine the likelihood and expected intensity of hiatus events in climate models as a function of the past global warming trend since the end of the nineteenth century and of four IPCC global warming scenarios for the next century [Taylor et al., 2012] (RCP2.6 and RCP4.5, two “stabilization scenarios,” RCP6.0, “intermediate scenario,” and RCP8.5, “business as usual”). Using exclusively climate model simulations from the CMIP5 (Coupled Model Intercomparison Project phase 5) [Taylor et al., 2012], this analysis follows a perfect model approach. This means that model biases [Wang et al., 2014; Kerkhoff et al., 2014; Menary et al., 2015], either in the SAT “forced” response [Marotzke and Forster, 2015] or misrepresentation of its “internal” variability [Davy and Eseau, 2014; England et al., 2014], are ignored. (We refer the reader to the Appendix A for further discussion on this fundamental assumption.) Together with hiatus events, the likelihood of surge events (faster than expected warming) and their expected intensity are also evaluated. In all cases, both global and local analyses are performed.

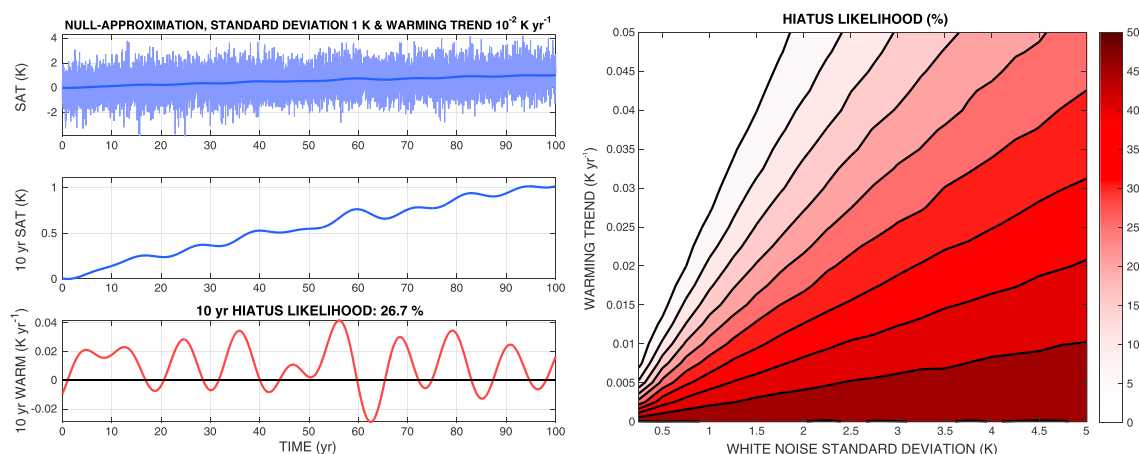


Figure 1. Null hypothesis. Statistics of decadal hiatus based on the null approximation (SAT is assumed to vary as white noise plus a linear trend). (top left) SAT as a centered white noise of 1 K standard deviation plus a linear warming trend of $10^{-2} \text{ K yr}^{-1}$. (middle left) SAT after a 10 year low-pass filter is applied (also plotted in dark blue in Figure 1, top left). (bottom left) Trend of 10 year low-pass-filtered SAT, decadal surge, and hiatus periods correspond to positive and negative values, respectively. The likelihood of decadal hiatus is the overall time spent in periods of negative trend (26.7%). (right) Sensitivity of the decadal hiatus likelihood to the two parameters of the null hypothesis: (i) standard deviation of the centered white noise and (ii) intensity of the linear trend warming. Depending on these two parameters, the likelihood of decadal hiatus goes from 0 to 50%.

2. Historical Likelihood of Global Events

We compare the warming and cooling due to “internally generated” decadal variability in control simulations (fixed present-day atmospheric composition and solar forcing) with the global “externally forced” SAT trend of Historical (1950–1998) and future scenario simulations (see Appendix A for a description of the computation of externally forced trends and of the multimodel density distribution of internally generated decadal trends). We obtain a global SAT trend of $0.94 \times 10^{-2} \text{ K yr}^{-1}$ for the 1950–1998 period. Hiatus and surge likelihood and expected intensity for 1950–1998 are evaluated through the normalized density distribution of warming and cooling longer than 10 years under the global warming scenario (Figure 2a). This leads to a likelihood of a hiatus of 31% with an expected intensity of $-1.4 \times 10^{-2} \text{ K yr}^{-1}$ and a likelihood of a surge of 48% with an expected intensity of $2.7 \times 10^{-2} \text{ K yr}^{-1}$ (Table 1). The remaining 21% of 10 year trends corresponds to a neutral warm state, where warming occurs but less intensively than the global warming trend. As expected under a global warming climate, surges are more likely and have a relatively more severe expected intensity than hiatus periods.

To further identify the likelihood and expected intensity of both hiatus and surge events, we generalize the previous analysis from 1860 to 2000 of the historical simulation. We follow the same methodology, but here the global decadal SAT trends are computed each year, as a multimodel mean of each historical simulation. By combining this “instantaneous” externally forced decadal trend with the multimodel mean normalized distribution of global warming and cooling, we diagnose the likelihood and expected intensity of hiatus and surge events all along the historical simulations (Figure 2b). We now obtain four types of events (described in Figure S1 in the supporting information): hiatus (decadal cooling faster than the decadal trend), surge (decadal warming faster than the decadal trend), neutral warm (decadal warming slower than the decadal trend), and

Table 1. Characteristics of Decadal Hiatus and Surge Events in the Multimodel Mean for the Historical Period (1950–1998) and the Four Future Scenarios (RCP2.6, RCP4.5, RCP6.0, and RCP8.5)

	Global Warming Trend	Hiatus Likelihood	Hiatus Expected Intensity	Surge Likelihood	Surge Expected Intensity	Skewness of Local Events
Historic	$0.94 \times 10^{-2} \text{ K yr}^{-1}$	31%	$-1.4 \times 10^{-2} \text{ K yr}^{-1}$	48%	$2.7 \times 10^{-2} \text{ K yr}^{-1}$	+28%
RCP2.6	$0.72 \times 10^{-2} \text{ K yr}^{-1}$	31%	$-1.6 \times 10^{-2} \text{ K yr}^{-1}$	48%	$2.4 \times 10^{-2} \text{ K yr}^{-1}$	-
RCP4.5	$1.8 \times 10^{-2} \text{ K yr}^{-1}$	16%	$-1.4 \times 10^{-2} \text{ K yr}^{-1}$	48%	$3.5 \times 10^{-2} \text{ K yr}^{-1}$	+86%
RCP6.0	$2.3 \times 10^{-2} \text{ K yr}^{-1}$	13%	$-1.2 \times 10^{-2} \text{ K yr}^{-1}$	48%	$4.0 \times 10^{-2} \text{ K yr}^{-1}$	-
RCP8.5	$4.1 \times 10^{-2} \text{ K yr}^{-1}$	2.7%	$-1.1 \times 10^{-2} \text{ K yr}^{-1}$	48%	$5.9 \times 10^{-2} \text{ K yr}^{-1}$	+100%

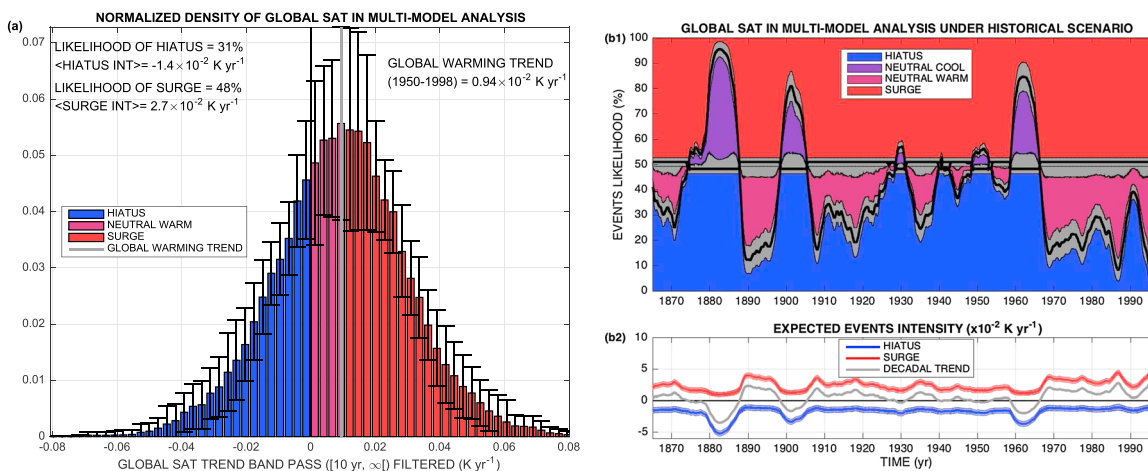


Figure 2. Distribution and historical characteristics of hiatus and surge events. (a) Normalized density distribution of events longer than 10 years for the historical (1950–1998) period. The histograms represent the multimodel mean of (blue) hiatus, (light purple) neutral warm, and (red) surge, whereas error bars represent the multimodel standard deviation. (b1) Evolution of decadal (red) surge, (dark purple) neutral cool, (light purple) neutral warm, and (blue) hiatus likelihood as a function of the historical decadal trend (evaluated through the multimodel historical scenario, grey curve in Figure 2b2). A hiatus is extremely unlikely after 1995. Grey shading represents the intermodel deviation. (b2) Surge (red) and hiatus (blue) expected intensity for the historical period, shaded regions represent multimodel standard deviation.

neutral cool (decadal cooling slower than the decadal trend). Neutral warm and cool events cannot coexist; their respective existence depends on the sign of the decadal trend (positive or negative, respectively). We find that during most of the historical period, surges are more likely (Figure 2b1). Hiatus has a significantly higher likelihood only during three periods: a decade around the 1880s, a decade around the 1900s, and a decade around the 1960s. From the early 1970s hiatus events are extremely unlikely, with a likelihood and expected intensity going to almost zero at the end of the 1990s. During this period surges have a likelihood of 50% with an increasing expected intensity, reaching a value of $\sim 5 \times 10^{-2} \text{ K yr}^{-1}$ in 1998 (Figure 2b2).

3. Future Likelihood of Global Events

We reproduce this analysis using four future scenarios (RCP2.6 and RCP4.5, two stabilization scenarios, RCP6.0, intermediate scenario, and RCP8.5, business as usual). We find that on average from 2000 to 2100, the global SAT trend is $0.72, 1.8, 2.3,$ and $4.1 \times 10^{-2} \text{ K yr}^{-1}$ for RCP2.6, RCP4.5, RCP6.0, and RCP8.5 (Table 1), respectively. In this context the hiatus likelihood decreases to 31%, 16%, 13%, and 2.7% whereas its expected intensity is roughly maintained at $-1.6, -1.4, -1.2,$ and $-1.1 \times 10^{-2} \text{ K yr}^{-1}$ for RCP2.6, RCP4.5, RCP6.0, and RCP8.5, respectively. On the other hand, surges show a constant likelihood at 48%, whereas their expected intensity increases to $3.5, 4.0,$ and $5.9 \times 10^{-2} \text{ K yr}^{-1}$ for RCP4.5, RCP6.0, and RCP8.5, respectively, but decreases to $2.4 \times 10^{-2} \text{ K yr}^{-1}$ for RCP2.6. Examining the evolution of these results along the 21st century (Figure 3), we find that RCP2.6 and RCP4.5 allow the recovery (in 2050 and 2100, respectively) of hiatus events comparable to surges for both likelihood (Figures 3a1 and 3b1) and expected intensity (Figures 3a2 and 3b2). RCP8.5 induces the disappearance of hiatus events with an increase of the expected intensity of surges up to $7.5 \times 10^{-2} \text{ K yr}^{-1}$ (Figures 3d1 and 3d2). On the other hand, the intermediate scenario, RCP6.0, shows relatively constant values of likelihood and expected intensity all along the 21st century, for both surge and hiatus events (Figures 3c1 and 3c2).

4. Historical and Future Likelihood of Local Events

Despite being instructive our global analysis is limited in its applicability because of the potentially strong spatial variations of the result. To overcome this difficulty, we reproduce the previous analyses at a local level on a generic $2^\circ \times 2^\circ$ grid (by applying linear interpolation from the native grid of each individual model). The first step is to compute the multimodel mean trend for the historical, RCP4.5, and RCP8.5 scenarios at a local level. (Here RCP2.6 and RCP6.0 are ignored, being qualitatively close to RCP4.5 and in between RCP4.5 and RCP8.5, respectively.) We obtain maps of SAT trend corresponding to a net warming over the historical period and under the two scenarios, with the classical polar amplification [Serreze and Francis, 2006; Bekryaev et al., 2010] especially visible for the North Pole (Figures 4a1–4a3). Warming is much stronger for RCP8.5 than

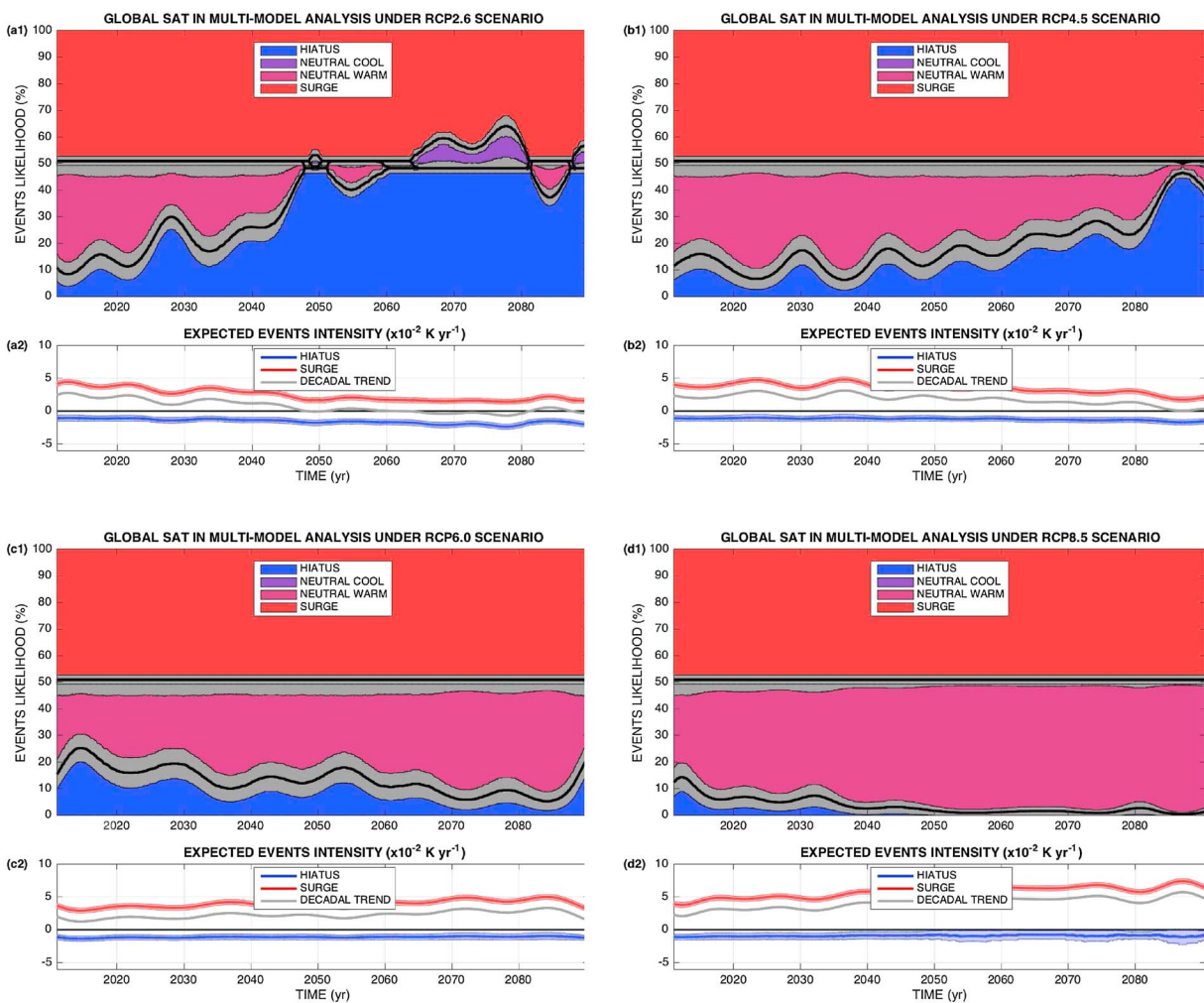


Figure 3. Characteristics of hiatus and surge events under future scenarios. As Figures 2b1 and 2b2 but for (a1 and a2) RCP2.6, (b1 and b2) RCP4.5, (c1 and c2) RCP6.0, and (d1 and d2) RCP8.5 decadal trend.

Historical, whereas RCP4.5 shows intermediate values. For all three cases, warming is stronger over land than over oceanic regions. After combining the multimodel mean statistic of local decadal events from the control simulations and the trend from the historical and the two future scenario simulations, we extract the local likelihood of hiatus and surge events as well as their respective expected intensity (Figure 5). Estimation of the error is given by the local multimodel standard deviations (Figure S2) and remains low compared to the mean values.

There are notable geographical differences. For all three scenarios, hiatus and surge events are more likely outside the subtropical oceans, with an intensification of likelihood in polar regions (Figures 5a1–5a3 and 5c1–5c3). Regarding the expected intensity, two bands centered around 70°S and 70°N show higher values than the rest of the globe (Figures 5b1–5b3 and 5d1–5d3).

There are also differences between the outcomes for the historical period and under the future scenarios. For hiatus events, the likelihood decreases between historical and warming scenarios (Figures 5a1–5a3), whereas the expected intensity remains constant (Figures 5b1–5b3). On the other hand, for surges, the likelihood is rather constant (Figures 5c1–5c3), and instead the expected intensity increases with the warming intensity of the scenario (Figures 5d1–5d3). However, in all cases the geographical patterns of likelihood and expected intensity for both hiatus and surge events barely change.

To qualitatively compare the likelihood of hiatus and surge events, we build an index measuring the skewness of events toward surge or hiatus (the difference between the local surge and hiatus likelihood, Figures 4b1–4b3). Hence, positive or negative values suggest regions biased toward surge or hiatus,

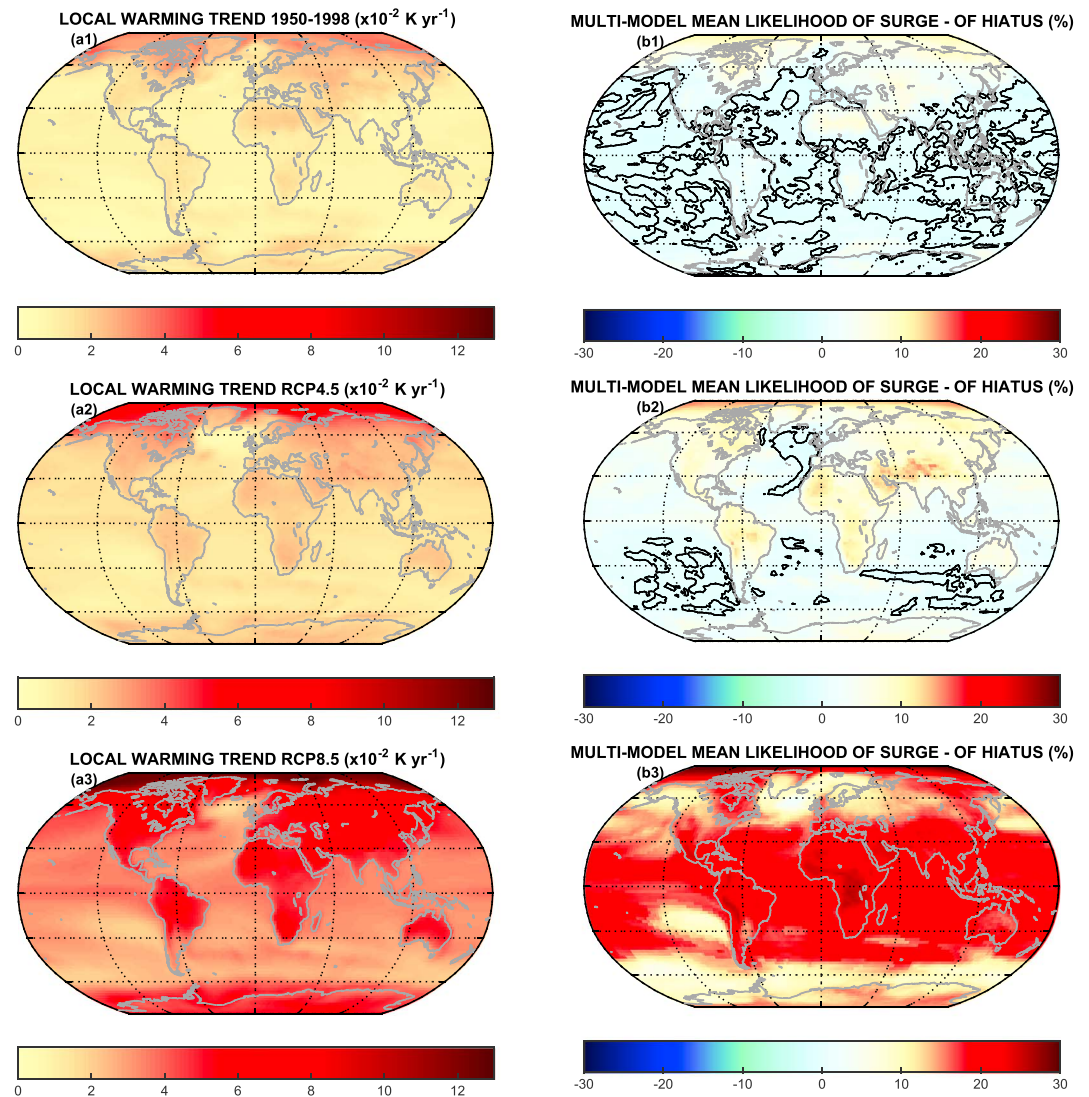


Figure 4. Local signature of global warming and local skewness between hiatus and surge. (a1–a3) Local warming and (b1–b3) difference of surge and hiatus likelihood, for (Figures 4a1 and 4b1) Historical (1950–1998), (Figures 4a2 and 4b2) RCP4.5, and (Figures 4a3 and 4b3) RCP8.5 scenarios. On the right-hand column (Figures 4b1–4b3), the black thick line represents the zero value (no skewness between hiatus and surge likelihood), $\pm 50\%$ suggests that all events are surge/hiatus at this location, respectively.

respectively, regardless of the expected intensity. Following this, the local skewness index is defined as ± 1 depending on whether surge or hiatus likelihood is larger (i.e., if their difference is positive or negative, respectively) and zero if the likelihoods are exactly equal. A global index is then defined as the spatial average of the local skewness index rescaled as % of the globe ($\pm 100\%$ suggests that the entire globe is biased toward surge/hiatus events). This last diagnostic suggests that during warmer scenarios, SAT is more intensely biased toward surge events, until 100% of the globe is biased toward surges for RCP8.5 (Table 1). At local scale, the index shows that oceanic regions are more susceptible to hiatus events than continents for the historical period (Figure 4b1). Under RCP4.5, only a few regions of the Southern Ocean are still biased toward hiatus, along with the northern and eastern parts of the North Atlantic, forming a “comma” shape in this region (Figure 4b2). This region, particularly susceptible to hiatus events, is linked to the constructive effect of the relative weak warming in the North Atlantic [Rahmstorf et al., 2015], potentially related to a slowdown of the Atlantic Meridional Overturning Circulation [Drijfhout et al., 2012] and the high-amplitude decadal variability of this region [Sévellec and Fedorov, 2013]. The rest of the globe is biased toward surges with intensification at the pole and over continental regions. Under RCP8.5, the whole globe is biased toward surges (Figure 4b3),

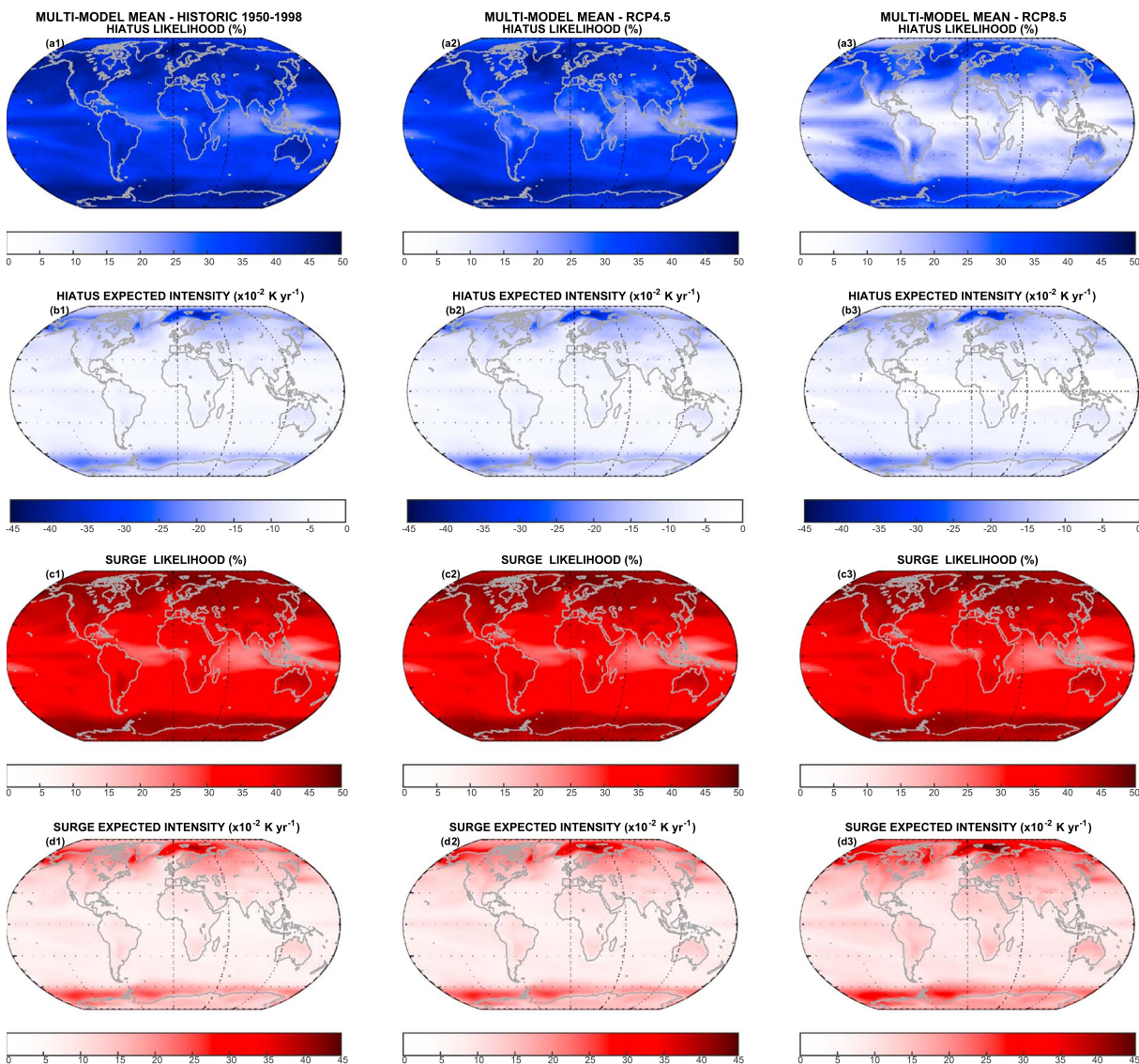


Figure 5. Local characteristics of hiatus and surge events. Hiatus (a1–a3) likelihood and (b1–b3) expected intensity and surge (c1–c3) likelihood and (d1–d3) expected intensity for (Figures 5a1, 5b1, 5c1, and 5d1) historical (1950–1998), (Figures 5a2, 5b2, 5c2, and 5d2) RCP4.5, and (Figures 5a3, 5b3, 5c3, and 5d3) RCP8.5 scenarios.

with a weaker bias over two bands centered around 60°S and 60°N, coincident with the midlatitude storm tracks.

5. Conclusion

From our multimodel analysis of historical and future likelihood of hiatus and surge events, we have found that the hiatus of the early 21st century appears to be extremely unlikely: likelihood less than 2%. This is consistent with previous analyses suggesting that only 10 CMIP5 members over 262 produce a decadal hiatus during this period [Meehl *et al.*, 2014]. We have also shown that the likelihood of hiatus events should decrease under an intensification of global warming but retain a constant expected intensity. On the other hand, the likelihood of surges should be steady with an increase of expected intensity. By the end of 21st century, an even expectancy of hiatus and surge events can be recovered under RCP2.6 and RCP4.5 (typical of the 1940s), whereas transient decadal cooling will be extremely unlikely under RCP8.5 (consistent with the previous study of Maher *et al.* [2014]). Our analysis also shows important spatial variability. Hiatus and surge events are expected to be more intense in polar regions and more likely over land and poleward of the tropics (equatorward of the tropics, the regime is more likely to be neutral). Furthermore, this spatial variability depends on the imposed

scenario. In the Historical simulations, midlatitude/tropical oceanic regions are skewed toward hiatus events, whereas land is skewed toward surges. Under RCP4.5, only the northeast Atlantic retains a significantly higher likelihood of hiatus than surges, and under RCP8.5, surges are more likely everywhere.

The extremely low likelihood (less than 2%) of early 21st century hiatus in this multimodel analysis raises some important questions. We can explain this apparent paradox through the formulation of three hypotheses:

1. Numerical models are hardly able (because of low decadal variability or too high climate sensitivity) to reproduce the hiatus [Fyfe *et al.*, 2013]. Therefore, there is an urgent need to develop improved climate models. This hypothesis is at the heart of our analysis (see Appendix A for further discussion).
2. Data collection is biased [Cowtan and Way, 2014; Karl *et al.*, 2015] toward regions of hiatus or moderate surge (tropics and midlatitudes) compared to regions of intense surge (e.g., polar regions), wrongly emphasizing/overestimating the hiatus of the early 21st century.
3. Numerical models and data collection are both correct so that the recent observed hiatus event was extremely unlikely. This hypothesis seems credible since both observations and numerical models lead to similar likelihood estimation [Schurer *et al.*, 2015]. In this context, given the significant impact of the recent hiatus on the perception of climate change by the public and according to the Black Swan Theory (i.e., the destructive impact of the occurrence of outlier events on the development of theory for classical events [Taleb, 2007]), there is a risk of inappropriate mistrust of current numerical models instead of acknowledging the highly unlikely nature of the event, at the limit of climate variability [Taleb, 2001]. This mistrust would be especially counterproductive, since this past rogue event has been shown to be fully captured by current prediction systems [Guemas *et al.*, 2013; Meehl *et al.*, 2014], demonstrating the relevance of operational decadal predictions.

In this context, it seems appropriate to be prepared for extreme events such as the hiatus of the early 21st century or surge “evil twin” events and continue to employ observations and numerical models to improve our understanding of climate variability, including, but not restricted to, the occurrence of extremes.

Appendix A: Method for the Multimodel Analysis

The analysis performed in this study followed a multimodel approach (i.e., all the statistics are estimated from ensemble averages of 20 climate models). The surface air temperature (SAT) data for control (with fixed present-day atmospheric greenhouse gas concentrations), historical, Representative Concentration Pathways 2.6, 4.5 (RCP2.6 and RCP4.5, two stabilization scenarios), 6.0 (RCP6.0, intermediate scenarios), and 8.5 (RCP8.5, business as usual) simulations were gathered from the CMIP5 database [Taylor *et al.*, 2012]. The 20 models are as follows: (1) IPSL-CM5A-MR, (2) CCSM4, (3) EC_EARTH, (4) GFDL-CM3, (5) MIROC5, (6) BNU-ESM, (7) CSIRO-MK3, (8) CanESM2, (9) MPI-ESM-MR, (10) INMCM4, (11) CNRM-CM5, (12) GISS-E2-R, (13) BCC-CSM1-1, (14) ACCESS1-3, (15) CMCC-CESM, (16) FGOALS-g2, (17) FIO-ESM, (18) MRI-CGCM3, (19) NorESM1-M, and (20) MOHC_HadGEM2-ES. Except for RCP8.5 some models were missing: for RCP2.6, (10), (14), and (15); for RCP4.5, (15); and for RCP6.0, (3), (4), (6), (8)–(11), (14)–(16), and (18).

To compute the likelihood and expected intensity of decadal hiatus and surge events, we build the normalized density distribution at both local and global scale for historical, RCP2.6, RCP4.5, RCP6.0, and RCP8.5 future scenarios. This density distribution is obtained by the linear combination of internal decadal variability assessed from the the control simulations and linear forced trends assessed from the historical and RCP scenarios.

To evaluate the decadal internal variability, we use SAT both globally (after a global spatial horizontal averaging) and locally (after linear interpolation from the respective native model grid to a regular $2^\circ \times 2^\circ$ grid) for each of the 20 models. The SAT is filtered using a low-pass filter with a cutoff frequency set at 10 years and based on a simple step function (i.e., removing all frequency components above the cutoff frequency but not affecting lower frequencies). A probability density function of the time derivative of this filtered SAT is built to represent the likelihood of warming and cooling events equal to or longer than 10 years (other minimum durations have been widely tested in Figure S3; for more exhaustive discussion on this point we refer the reader to Medhaug and Drange [2015]). The decadal internal density distribution is evaluated through the 20-model mean.

Note that this definition of events differs from Roberts *et al.* [2015] and Schurer *et al.* [2015], for example. In these two studies the events are defined with a specific timescale (versus a timescale greater than a fixed

threshold). This implies that our results are the integral of theirs. Hence, despite using the same methodology to assess events likelihood, direct numerical comparison with these studies is not possible. We chose our definition because of its broader property, defining long enough events (to disregard interannual/short events with weaker climatic impact) without restricting to a specific timescale.

Linear trends are evaluated using a linear regression of both global and local SAT (for the decadal trend we used 5 years before and after) for historical, RCP2.6, RCP4.5 RCP6.0, and RCP8.5. The forced linear trend corresponds to the 20-model mean. This allows the removal of out-of-phase internal decadal variability, hence limiting its impact on the linear trend (grey lines in Figures 2b2 and 3a2–3d2 do not exhibit high decadal variability). We chose to use a single realization for each model, and not all the different initial condition members where available, to avoid biasing our study toward the models which were run with a large number of ensemble members.

Finally, assuming a linear combination of the forced linear trend from historical, RCP2.6, RCP4.5 RCP6.0, and RCP8.5 simulations and of the internal variability of the control simulations, we construct the normalized density distribution of warming and cooling events longer than 10 years under historical and different future global warming scenarios. We do this by centering the distribution of internal variability obtained from the control simulation on the forced linear trend obtained from historical and RCP scenarios.

In this framework, a hiatus can be partially generated from the forced variability (through solar changes or volcanic eruptions, for instance) and the decadal internal variability acts to reinforce or suppress this forced hiatus.

It is important to stress that this entire analysis is based on a perfect model approach. Here model biases [Wang *et al.*, 2014; Kerkhoff *et al.*, 2014; Menary *et al.*, 2015] arising either from a misrepresentation of the forced linear trend or from inaccurate internal variability compared to observations are ignored. Whereas there is no indication of potential issues with the former [Marotzke and Forster, 2015], there is evidence of low decadal variability in numerical models [Davy and Eseau, 2014]. For example, the intensity of Pacific trade wind variations, potentially essential for the recent hiatus, is significantly biased between CMIP5 models and observations [England *et al.*, 2014]. These modelling shortcoming would inherently affect our analysis, suggesting that our results could have underestimated the likelihood of hiatuses and the expected intensity of surges.

Acknowledgments

This research was supported by the Natural and Environmental Research Council UK (MESO-CLIP, NE/K005154/1 and SMURPHS, NE/N005767/1 and NE/M005686/1). The authors acknowledge the World Climate Research Programme's Working Group on Coupled Modelling, which is responsible for CMIP, and we thank the climate modeling groups for producing and making available their model output (listed in Appendix A of this paper). For CMIP the U.S. Department of Energy's Program for Climate Model Diagnosis and Intercomparison provides coordinating support and led development of software infrastructure in partnership with the Global Organization for Earth System Science Portals.

References

- Balmaseda, M. A., K. E. Trenberth, and E. Källén (2013), Distinctive climate signals in reanalysis of global ocean heat content, *Geophys. Res. Lett.*, *40*, 1754–1759, doi:10.1002/grl.50382.
- Bekryaev, R. V., I. V. Polyakov, and V. A. Alexeev (2010), Role of polar amplification in long-term surface air temperature variations and modern arctic warming, *J. Clim.*, *23*, 3888–3906.
- Clement, A., and P. DiNezio (2014), The tropical pacific ocean — Back in the driver's seat?, *Science*, *343*, 976–978.
- Cowan, K., and R. G. Way (2014), Coverage bias in the HadCRUT4 temperature series and its impact on recent temperature trends, *Q. J. R. Meteorol. Soc.*, *140*, 1935–1944.
- Davy, R., and I. Eseau (2014), Global climate models' bias in surface temperature trends and variability, *Environ. Res. Lett.*, *9*, 114024.
- Drijfhout, S., G. J. van Oldenborgh, and A. Cimadoribus (2012), Is a decline of AMOC causing the warming hole above the North Atlantic in observed and modeled warming patterns?, *J. Clim.*, *25*, 8373–8379.
- Drijfhout, S., A. T. Blaker, S. A. Josey, A. G. J. Nurser, B. Sinha, and M. A. Balmesada (2014), Surface warming hiatus caused by increased heat uptake across multiple ocean basins, *Geophys. Res. Lett.*, *41*, 7868–7874, doi:10.1002/2014GL061456.
- Easterling, D. R., and M. F. Wehner (2009), Is the climate warming or cooling?, *Geophys. Res. Lett.*, *36*, L08706, doi:10.1029/2009GL037810.
- England, M. H., S. McGregor, P. Spence, G. A. Meehl, A. Timmermann, W. Cai, A. S. Gupta, M. J. McPhaden, A. Purich, and A. Santoso (2014), Recent intensification of wind-driven circulation in the Pacific and the ongoing warming hiatus, *Nat. Clim. Change*, *4*, 222–227.
- England, M. H., J. B. Kajtar, and N. Maher (2015), Robust warming projections despite the recent hiatus, *Nat. Clim. Change*, *5*, 394–396.
- Fyfe, J. C., N. P. Gillett, and F. W. Zwiers (2013), Overestimated global warming over the past 20 years, *Nat. Clim. Change*, *3*, 767–769.
- Guemas, V., F. J. Doblas-Reyes, I. Andreu-Burillo, and M. Asif (2013), Retrospective prediction of the global warming slowdown in the past decade, *Nat. Clim. Change*, *3*, 649–653.
- IPCC (2013), *Climate Change 2013 — The Physical Science Basis: Contribution of Working Group I to the Fifth Assessment Report of the IPCC*, Cambridge Univ. Press, Cambridge, U. K.
- Karl, T. R., A. Arguez, B. Huang, J. H. Lawrimore, J. R. McMahon, M. J. Menne, T. C. Peterson, R. S. Vose, and H.-M. Zhang (2015), Possible artifacts of data biases in the recent global surface warming hiatus, *Nature*, *388*, 1469–1472.
- Katsman, C. A., and G. J. Oldenborgh (2011), Tracing the upper ocean's "missing heat", *Geophys. Res. Lett.*, *38*, L14610, doi:10.1029/2011GL048417.
- Kerkhoff, C., H. R. Künsch, and C. Schär (2014), Assessment of bias assumptions for climate models, *J. Clim.*, *27*, 6799–6818.
- Maher, N., A. Sen Gupta, and M. H. England (2014), Drivers of decadal hiatus periods in the 20th and 21st centuries, *Geophys. Res. Lett.*, *41*, 5978–5986, doi:10.1002/2014GL060527.
- Marotzke, J., and P. Forster (2015), Forcing, feedback and internal variability in global temperature trends, *Nature*, *517*, 565–570.
- Medhaug, I., and H. Drange (2015), Global and regional surface cooling in a warming climate: A multi-model analysis, *Clim. Dyn.*, *46*, 3899–3920, doi:10.1007/s00382-015-2811-y.

- Meehl, A. G., J. Arblaster, J. Fasulo, A. Hu, and K. E. Trenberth (2011), Model-based evidence of deep-ocean heat uptake during surface-temperature hiatus periods, *Nat. Clim. Change*, *1*, 360–364.
- Meehl, G. A., A. Hu, J. Arblaster, J. Fasulo, and K. E. Trenberth (2013), Externally forced and internally generated decadal climate variability associated with the interdecadal Pacific oscillation, *J. Clim.*, *26*, 7298–7310.
- Meehl, G. A., H. Teng, and J. M. Arblaster (2014), Climate model simulations of the observed early-2000s hiatus of global warming, *Nat. Clim. Change*, *4*, 898–902.
- Menary, M. B., D. L. R. Hodson, J. I. Robson, R. T. Sutton, R. A. Wood, and J. A. Hunt (2015), Exploring the impact of CMIP5 model biases on the simulation of North Atlantic decadal variability, *Geophys. Res. Lett.*, *42*, 5926–5934, doi:10.1002/2015GL064360.
- Rahmstorf, S., J. E. Box, G. Feulner, M. E. Mann, A. Robinson, S. Rutherford, and E. J. Schaffernicht (2015), Exceptional twentieth-century slowdown in Atlantic ocean overturning circulation, *Nat. Clim. Change*, *5*, 475–480.
- Rajaratnam, B., J. Romano, M. Tsiang, and N. S. Diffenbaugh (2015), Debunking the climate hiatus, *Clim. Change*, *133*, 129–140.
- Risbey, J. S., S. Lewandowsky, J. R. Hunter, and D. P. Monselesan (2015), Betting strategies on fluctuations in the transient response of greenhouse warming, *Philos. Trans. R. Soc. A*, *373*, 14, doi:10.1098/rsta.2014.0463.
- Roberts, C. D., M. D. Palmer, D. McNeall, and M. Collins (2015), Quantifying the likelihood of a continued hiatus in global warming, *Nat. Clim. Change*, *5*, 337–342.
- Schurer, A. P., G. C. Hegerl, and S. P. Obrochta (2015), Determining the likelihood of pauses and surges in global warming, *Geophys. Res. Lett.*, *42*, 5974–5982, doi:10.1002/2015GL064458.
- Serreze, M. C., and J. A. Francis (2006), The arctic amplification debate, *Clim. Change*, *76*, 241–264.
- Sévellec, F., and A. V. Fedorov (2013), The leading, interdecadal eigenmode of the Atlantic meridional overturning circulation in a realistic ocean model, *J. Clim.*, *26*, 2160–2183.
- Taleb, N. N. (2001), *Foiled by Randomness: The Hidden Role of Chance in Life and in the Markets*, 316 pp., Random House.
- Taleb, N. N. (2007), *The Black Swan: The Impact of the Highly Improbable*, 400 pp., Random House.
- Taylor, K. E., R. J. Stouffer, and G. A. Meehl (2012), An overview of CMIP5 and the experiment design, *Bull. Am. Meteorol. Soc.*, *93*, 485–498.
- Trenberth, K. E. (2015), Has there been a hiatus?, *Science*, *349*, 691–691.
- Trenberth, K. E., and J. T. Fasullo (2013), An apparent hiatus in global warming?, *Earth's Future*, *1*, 19–32.
- Wang, C., L. Liping Zhang, S.-K. Lee, L. Wu, and C. R. Mechoso (2014), A global perspective on CMIP5 climate model biases, *Nat. Clim. Change*, *4*, 201–205.
- Watanabe, M., Y. Kamae, M. Yoshimori, A. Oka, M. Sato, M. Ishii, T. Mochizuki, and M. Kimoto (2013), Strengthening of ocean heat uptake efficiency associated with the recent climate hiatus, *Geophys. Res. Lett.*, *40*, 3175–3179, doi:10.1002/grl.50541.